Filtering of systems with heavy tailed noise: application to 3D target tracking with glint noise

Stefano Battilotti, Filippo Cacace, Massimiliano d'Angelo, Emanuele Della Corte, and Alfredo Germani

Abstract—**In this paper a filtering method for non-Gaussian linear systems is adopted to face the problem of the target tracking in the presence of the glint noise. In particular, we extend the quadratic filtering method with virtual measurements to the three-dimensional case of the target tracking problem. Moreover, we present extensive numerical simulation by comparing our method with several filtering algorithms used in the case of heavy tailed noises. The latter numerical results confirm the effectiveness of the proposed approach.**

Keywords: target tracking; Kalman filtering; heavy tailed noise; glint noise; non-Gaussian systems.

I. INTRODUCTION

In this paper we are interested in the problem of state estimation for radar target tracking in the presence of heavy tailed noises, in particular the glint noise, which is a non-Gaussian noise that appear in Aerospace applications ([1]). The addressed problem consists in dealing with the filtering of noisy data retrieved from the measurements of the position, velocity and acceleration of an object tracked by a radar. In fact, under some conditions depending on the physical structure of the object to be tracked, the output of the radar may give readings which are particularly misleading, in a way which is really difficult to cope with. In [2], [3] it is introduced a nonlinear score function as a correction term in the state estimate, in the works [4], [5], [6] Kalman filtering techniques are developed, while particle filter-based methodologies are deepened in the works [7], [8], [9], [10], [11] and a Maximum Likelihood identification method for the Gaussian-Laplacian mixture was proposed in [12]. Another layer of complexity is added for the modeling of the glint noise. Several methods have been and are being developed and applied in order to filter the noisy measurements, and a relatively wide state-of-the-art showing solutions to glint noise filtering can be found in the literature. Yet many common methods, even showing relatively satisfactory results, return far-to-optimal solutions.

The approach proposed here is based on the recursive quadratic estimator of [13], [14] and [15]. In particular, the contribution of this work is the construction of the latter estimator for the 3D case of the target tracking problem in glint noise environment. Moreover, we present extensive numerical simulations and comparisons with standard approaches. The main advantage of this approach is to retain the benefits of linear filters, like internal stability of the filter and the computation of the variance of the state estimation error together with better performance.

Theory of glint noise in target tracking

The nature of radar systems have been largely investigated in the works [16], [17]. A radar is an electromagnetic system whose aim is the detection and the location of objects. A radar basic principle consists in the emission of radiating electromagnetic energy and the detection of the echoes returned from the object to be tracked. However, in a target tracking environment there are numerous sources of noise. The most troublesome sources of noise are the ones which cannot be avoided in any case, since they arise from the physical structure of the object to be tracked. Since the target position changes in time, the superposition rises unexpectedly in time, which is the reason why the nature of such errors is stochastic. A particular kind of fluctuation in the measured angle is the angle glint, also called *target glint noise*. The effect of this distortion is a deviation on the computation over the apparent angle of the tracked object, as discussed in [1], so that it is read a wandering of the object with respect to the true position. The state-of-the-art regarding the modeling of glint noise is indeed still a work in progress. What is well-known, as stated in the work [18], is the experimentally-obtained power spectrum of the noise affecting the measurements and its heavily non-Gaussian behaviour. Such power spectrum expresses a record of a background component which is strongly dominating with respect to a second behavior which appears in the form of a certain random number of spikes as it is possible to highlight in Figure 1.

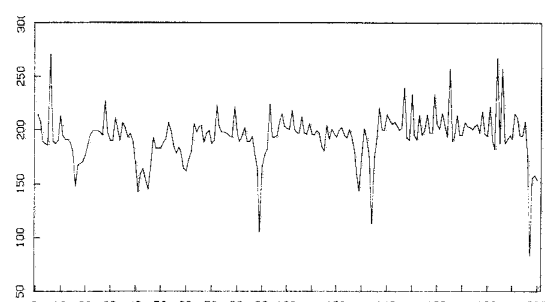

Fig. 1. A typical glint noise record ([4])

Stefano Battilotti battilotti@diag.uniroma1.it is with the Department of Computer Control and Menagement Engineering (DIAG), Sapienza University of Rome.

Filippo Cacace f.cacace@unicampus.it is with Università Campus Bio-medico di Roma, Italy.

Massimiliano d'Angelo massimiliano.dangelo@unimib.it is with the Department of Biotechnology and Biosciences (BtBs), University of Milano-Bicocca.

Emanuele Della Corte dellacorte.e@fatergroup.com is a Digital Process Engineer at Fater S.p.A .

Alfredo Germani germani@ing.univaq.it is with the Dipartimento di Ingegneria e Scienze dell'Informazione e Matematica, Università dell'Aquila, Italy.

In this work glint noise will be modeled as a Gaussian-Laplacian mixture. This idea has been supported for instance in the work [19], so that the resulting probability density function is described by

$$p(x) = \varepsilon p_L(x) + (1 - \varepsilon) p_G(x) \tag{1}$$

where ε is the occurrence probability of the Laplacian noise, and:

$$p_G(x) := \mathcal{N}(x; 0, \sigma_G^2) := \frac{1}{\sqrt{2\pi}\sigma_G} e^{-\frac{x^2}{2\sigma_G^2}}$$

$$p_L(x) := \mathcal{L}(x; 0, \sigma_L^2) := \frac{1}{2\eta} e^{-\frac{|x|}{\eta}}$$

with η such that $2\eta^2 = \sigma_L^2$.

The paper is organised as follows. We recall some existing concepts on quadratic filtering and the virtual measurement approach in Section II. The 2D and 3D target tracking equations are derived in Section II-B. Numerical simulations and comparisons are presented in Section IV and conclusions follow.

Notation. The symbol $\otimes$ denotes the Kronecker product between vector or matrices. The n-th Kronecker power of A is $A^{[n]}$. For a stochastic vector $v \in \mathbb{R}^n$, $\mathbb{E}[v]$ is the expectation, Ψ_v the covariance matrix and $\Psi_v^{(i)} = \mathbb{E}[v^{[i]}] \in \mathbb{R}^{n^i}$ the expected value of its n-th Kronecker power. The spectrum of a square matrix A is $\sigma(A)$.

II. Quadratic filtering and Virtual measurement approach

In this section we recall some existing results in the context of filtering of non-Gaussian systems [13] and the so-called *virtual measurement map* [15] that will be instrumental for the application to the target tracking problem. We refer the interested reader to those papers for further details.

A. Quadratic filtering

In the context of linear non-Gaussian systems it is possible to use quadratic (or in general polynomial) functions of the observations to improve the estimation accuracy while preserving easy computability and recursion ([13], [14]). In few words, this approach consists in obtaining a sub-optimal quadratic estimate by applying the Kalman Filter to an augmented system that contains the second order (Kronecker) powers of the state and of the observations.

This technique applies to a discrete-time linear system with non-Gaussian noise in the form

$$x(k+1) = Ax(k) + f_k, \quad x(0) = x_0 \tag{2}$$

$$y(k) = Cx(k) + g_k \tag{3}$$

where $x(k) \in \mathbb{R}^n$, $y(k) \in \mathbb{R}^p$, $A \in \mathbb{R}^{nxn}$, $C \in \mathbb{R}^{qxn}$. $\{f_k\}$ and $\{g_k\}$ are sequences of non-Gaussian random variables with values in $\mathbb{R}^n$ and $\mathbb{R}^q$, respectively. The systems is assumed to be fully observable. The random sequences $\{f_k\}$ and $\{g_k\}$ and the initial random variable x_0 are required to satisfy the following conditions $\forall k \geq 0$:

- $x_0 \sim \mathcal{N}(\bar{x}_0, \psi_{x_0})$
- $\{f_k\}$ and $\{g_k\}$ are sequences of zero mean temporally independent random vectors.
- x_0, f_k and g_k have finite fourth moments.
- $\psi_{x_0}^{(i)}, \psi_f^{(i)}, \psi_g^{(i)}$, $i = 2, 3, 4$, are known vectors.
- $[C\ \psi_g], \psi_g = st_q^{-1}(\psi_g^{(2)})$ is full row rank (FRR).

The idea is to obtain a state estimation by projecting the state $x(k)$ onto larger subspace w.r.t. the subspace of affine transformations of the measurement vector. Here, we consider the space of quadratic transformations of

$$\bar{Y}_k^{(2)} = (Y_k^{'}, y(0)^{[2]}, ..., y(k)^{[2]}),\ Y_k := (y(0), y(1), \ldots, y(k))^\top$$

where the mixed-products at different time are not considered. The new projection space will be then:

$$\bar{\mathcal{Q}}_y^k = \left\{ z : \Omega \to \mathbb{R}^n :\ \exists T \in \mathbb{R}^{n\ \text{x}\ \bar{l}} : z = T\bar{Y}_k^{(2)} \right\} \tag{4}$$

The obtained *recursively computable* quadratic estimate $\hat{x}$ will not be the optimal quadratic estimate, but will still be closer to optimality than the affine one. We shall call this filter *Feedback Quadratic Filter* (FQF).

In the next section, we show how to extend the application of this filter to systems with nonlinear measurements ([15]). The application of this methodology to target tracking problems is an intuition which dates back to some of the earliest investigations on target tracking, as it can be deepened in the work [20] and in the survey [21]. To the obtained linear system, a standard Kalman Filter procedure can finally be carried on.

B. Virtual Measurement approach

In the case of target tracking the measurements of the target are tipically nonlinear (distance and angle). In fact, instead of the measurement equation (3) we consider

$$y(k) = h(Cx(k)) + v_k \tag{5}$$

where the matrix $C \in \mathbb{R}^{\tilde{n}\ \text{x}\ n}$ determines the portion of the state involved in the, possibly nonlinear, measurement map. The discrete-time noise sequence $\{v_k\}$ is zero-mean i.i.d. and same assumptions as before hold true. We point out that the measurement noise sequence $\{v_k\}$ (as also for $\{f_k\}$) is not restricted to have a Gaussian distribution. In particular, in our case of interest, the sequence $\{v_k\}$ is characterized by the glint noise, which is an heavy tailed (non-Gaussian) noise (see Section I).

The final goal is extracting a linear measurement equation through an output transformation. In particular, it is given the following definition ([15]).

Definition 1: System (5) admits a linear representation of the measurement map if there are $\Gamma : \mathbb{R}^q \to \mathbb{R}^{q_v}$, $\Psi : \mathbb{R}^q \ \text{x}\ \mathbb{R}^q \to \mathbb{R}^{q_v}$ and a constant matrix $C_v \in \mathbb{R}^{q_v\ \text{x}\ n}$ with $q_v \geq q$ such that, for any $k \geq 0$:

$$y_v(k) = C_v x(k) + g_k, \tag{6}$$

where $y_v(k) := \Gamma(y(k)), \quad g_k := \Psi(y(k), v_k)$.

The obtained output $y_v(k)$ is said to be the linear-transformed output. A further characterization rises for the case in which

the observability matrix $\mathcal{O}(A, C_v)$ has full rank: if so, the system (2) together with the nonlinear measurement equation (5) admits an observable linear representation of the measurement map.
The virtual measurement map is recovered based on the following definition. II:

Definition 2: Be $z \in \mathbb{R}^{n_z}$ a random vector with probability density function f_z, let $\theta \in \mathbb{R}^{n_\theta}$ be a known parameter and $\eta : \mathbb{R}^{n_\theta}$ x $\mathbb{R}^{n_z} \rightarrowtail \mathbb{R}^{n_\eta}$ an integrable function. The moments of order i of $\eta(\theta, z)$ are defined as:

$$m_i[\eta] := \int_\Omega \eta^{[i]} dP(\omega) = \int_{\mathbb{R}^{n_z}} \eta(\theta, \tau)^{[i]} f_z(\tau) d\tau \tag{7}$$

Assuming now the following assumptions:

1) $\mathcal{O}(A, C)$ is full rank.
2) The function $h(\cdot)$ is invertible with known $h^{-1}(\cdot)$ in the domain of interest.

For the case $\tilde{n}$ = q, the virtual measurement map transformation is found as:

$$y_v(k) = \Gamma(y(k)) := m_1\left[h^{-1}(y(k) - v_k)\right] \tag{8}$$

Proposition 1: If $\tilde{n} = q$ and the assumptions 1 and 2 hold true, then (8) is an observable linear representation of the measurement map for the system (5) with $q_v = q$, $C_v = C$ and:

$$g_k = \Psi(y(k), v_k) := -h^{-1}(y(k) - v_k) + m_1\left[h^{-1}(y(k) - v_k)\right]$$

where $m_1[g_k] = 0$ and $m_1[g_k g_j^T] = 0$ for $k \neq j$.
We point out that this transformation map is not a *linearization* of the system (as it happens for instance in the EKF procedure). Thus, one may benefit of a much faithfulness of the model to the system and provide a more accurate stability analysis together with designing algorithm with better performance.

III. 2D AND 3D TARGET TRACKING

A target tracking problem is generally described by the system (2) and (5), moreover it satisfies the Proposition 1, *i.e.* it admits a linear observable representation of the measurement map. The idea is to apply the standard procedure of virtual measurement map and exploit the definitions of polar to cartesian change of coordinates in order to recover a linear representation of the original system.

A. 2D virtual measurement map

The literature provides several ways of modeling a target tracking problem, which must be defined as accurate as possible in order to capture the evolution of the dynamical features of the object to be tracked, which are usually hardly identifiable and unknown. The model of target tracking which is here used is the one introduced in the previous section. In particular, in a two-dimensional target tracking problem the characteristics of the object to be tracked can be described by the state vector $x(k) \in \mathbb{R}^6$ with $(x_1(k),\ x_4(k))$ being the position in the plan at step k, $(x_2(k),\ x_5(k))$ and $(x_3(k),\ x_6(k))$ being respectively the velocity and the acceleration vector. In the present work, a Constant velocity (CV) model is used to model the dynamics of the state. Consider $A = \text{diag}(\bar{A}, \bar{A})$, *i.e.* define as $\bar{A}$ the state matrix for each component in the space, and be $F \in \mathbb{R}^{n \text{ x } p}$ a matrix such that $w_k = F\tilde{w}_k$ where $\tilde{w}_k \sim \mathcal{N}(0, I_p)$ such that $F = \text{diag}(\bar{F}, \bar{F})$. Calling σ_a the acceleration standard deviation and τ the discretization step, the CV model is defined as the following:

$$\bar{A} = \begin{bmatrix} 1 & \tau & \frac{(\tau)^2}{2} \\ 0 & 1 & \tau \\ 0 & 0 & 0 \end{bmatrix} \qquad \bar{F} = \sigma_a \begin{bmatrix} 0 \\ 0 \\ 1 \end{bmatrix}. \tag{9}$$

Regarding the nonlinear measurements, defined as $\rho(k)$ and $\theta(k)$ respectively the distance and the angular position at time k, the output vector at time k in (5) is of dimension 2 and it follows:

$$y(k) = h(Cx(k)) = \begin{bmatrix} y_1(k) \\ y_2(k) \end{bmatrix} = \begin{bmatrix} \rho(k) \\ \theta(k) \end{bmatrix} + \begin{bmatrix} \varepsilon_{\rho,k} \\ \varepsilon_{\theta,k} \end{bmatrix} \tag{10}$$

where:

$$\rho(k) = \sqrt{x_1^2(k) + x_4^2(k)} \tag{11}$$

$$\theta(k) = \text{atan2}(x_4(k), x_1(k)) \tag{12}$$

The sequences $\varepsilon_{\rho,k}$ and $\varepsilon_{\theta,k}$ are zero-mean noises sampled from the glint noise probability density function introduced in (1). Details on the parameters of the latter density will be defined in Section IV. The numerical computations for the bi-dimensional case are left to the reader, whereas the tri-dimensional case is discussed in the next section. Notice that, the measurement equation (10) can be rewritten into a virtual linear stochastic equivalent system of the form (6) with $C_v = \begin{pmatrix} 1 & 0 & 0 & 0 & 0 & 0 \\ 0 & 0 & 0 & 1 & 0 & 0 \end{pmatrix}$. We recall that the state noise sequence $\{f_k\}$ is a Gaussian zero-mean noise sequence, whilst the obtained output noise $\{g_k\}$ is a transformation of the the glint noise v_k and it is a non-Gaussian zero-mean non-stationary noise sequence.

B. 3D virtual measurement map

We still consider for the 3D case the dynamical system of the CV model with nonlinear measurements affected by a general non-Gaussian noise sequence. The state space vector is defined on the space $x(k) \in \mathbb{R}^n = \mathbb{R}^9$, being $(x_1(k), x_4(k), x_7(k))$ the position vector, $(x_2(k), x_5(k), x_8(k))$ the velocity vector and $(x_3(k), x_6(k), x_9(k))$ the acceleration vector.
The state matrix $A \in \mathbb{R}^{9 \text{ x } 9}$ is defined as $A = \text{diag}(\bar{A}, \bar{A}, \bar{A})$. The noise matrix $F \in \mathbb{R}^{9 \text{ x } 3}$ is instead defined as $F = \text{diag}(\bar{F}, \bar{F}, \bar{F})$. The nonlinear measurements equation (5) in the 3D space are composed now also by the definition of the bearing angle ϕ:

$$y(k) = \begin{bmatrix} \sqrt{x_1^2(k) + x_4^2(k) + x_7^2(k)} \\ \text{atan2}(x_4, x_1) \\ \arccos\left(\frac{x_7(k)}{\sqrt{x_1^2(k)+x_4^2(k)+x_7^2(k)}}\right) \end{bmatrix} + \begin{bmatrix} \varepsilon_{\rho,k} \\ \varepsilon_{\theta,k} \\ \varepsilon_{\phi,k} \end{bmatrix} \tag{13}$$

$$= \begin{bmatrix} \rho(k) \\ \theta(k) \\ \phi(k) \end{bmatrix} + \begin{bmatrix} \varepsilon_{\rho,k} \\ \varepsilon_{\theta,k} \\ \varepsilon_{\phi,k} \end{bmatrix}. \tag{14}$$

The inverse mapping from spherical to Cartesian coordinates at time $k \geq 0$ follows the equations

$$\begin{aligned} x_1(k) &= \rho(k)\sin(\theta(k))\cos(\phi(k)), \\ x_4(k) &= \rho(k)\sin(\theta(k))\sin(\phi(k)), \\ x_7(k) &= \rho(k)\cos(\theta(k)). \end{aligned} \tag{15}$$

From (13), equations in (15) can be rewritten as

$$\begin{aligned} x_1(k) &= (y_1(k)-\varepsilon_{\rho,k})\sin(y_2(k)-\varepsilon_{\theta,k})\cos(y_3(k)-\varepsilon_{\phi,k}), \\ x_4(k) &= (y_1(k)-\varepsilon_{\rho,k})\sin(y_2(k)-\varepsilon_{\theta,k})\sin(y_3(k)-\varepsilon_{\phi,k}), \\ x_7(k) &= (y_1(k)-\varepsilon_{\rho,k})\cos(y_2(k)-\varepsilon_{\theta,k}). \end{aligned} \tag{16}$$

Define now

$$\begin{aligned} y_{v,1}(k) &= y_1(k)m_1[\sin(y_2(k)-\varepsilon_{\theta,k})\cos(y_3(k)-\varepsilon_{\phi,k})], \\ y_{v,2}(k) &= y_1(k)m_1[\sin(y_2(k)-\varepsilon_{\theta,k})\sin(y_3(k)-\varepsilon_{\phi,k})], \\ y_{v,3}(k) &= y_1(k)m_1[\cos(y_2(k)-\varepsilon_{\theta,k})], \end{aligned} \tag{17}$$

which entails the linear transformation. Finally, calling $\{g_k\}$ the new noise sequence defined by:

$$\begin{aligned} g_{1,k} = y_1(k)\big(&m_1[\sin(y_2(k)-\varepsilon_{\theta,k})\cos(y_3(k)-\varepsilon_{\phi,k})]+ \\ &-\sin(y_2(k)-\varepsilon_{\theta,k})\cos(y_3(k)-\varepsilon_{\phi,k})\big)+ \\ &+\varepsilon_{\rho,k}\big(\sin(y_2(k)-\varepsilon_{\theta,k})\cos(y_3(k)-\varepsilon_{\phi,k})\big) \\ g_{2,k} = y_1(k)\big(&m_1[\sin(y_2(k)-\varepsilon_{\theta,k})\sin(y_3(k)-\varepsilon_{\phi,k})]+ \\ &-\sin(y_2(k)-\varepsilon_{\theta,k})\sin(y_3(k)-\varepsilon_{\phi,k})\big)+ \\ &+\varepsilon_{\rho,k}\big(\sin(y_2(k)-\varepsilon_{\theta,k})\sin(y_3(k)-\varepsilon_{\phi,k})\big) \\ g_{3,k} = y_1(k)\big(&m_1[\cos(y_2(k)-\varepsilon_{\theta,k})]-\cos(y_2(k)-\varepsilon_{\theta,k})\big)+ \\ &+\varepsilon_{\rho,k}(\cos(y_2(k)-\varepsilon_{\theta,k}) \end{aligned} \tag{18}$$

one obtains again the equivalent linear system with Gaussian state noise sequence $\{f_k\}$ and zero-mean non-Gaussian non-stationary output noise sequence $\{g_k\}$, which is the final equivalent transformation. We point out again that also the orginal noise sequence $\{v_k\}$ is a non-Gaussian sequence (the glint noise).

IV. Numerical simulations and comparisons

The algorithm for the Feedback Quadratic Filter (FQF) introduced in Section II is implemented for the virtual measurement mapping developed in the previous section. In order to show the advantages of the proposed approach, we make a comparison with other existing solutions that are generally applied in the context of non-Gaussian systems. The results will be mainly compared in terms of estimation accuracy (and computational time).

A. Numerical simulations: 2D target tracking

All the simulation scenarios will share the same parameters regarding the initial state, the state noise and the glint noise. The initial state is

$$x_0 = \left[1000, -5, 0, -1000, 5, 0\right]^\top. \tag{19}$$

The noise sequence is defined as $f_k \sim \mathcal{N}(0, \sigma_f^2 I_2)$, where $\sigma_f^2 = 5\cdot 10^{-2}$. Concerning the measurement noise covariances, the covariance matrix for the background Gaussian measurement noise and the glint-noise matrix covariance are

$$\Sigma_g = \begin{pmatrix} 5 & 0 \\ 0 & 0.1 \end{pmatrix}, \; \Sigma_l = \begin{pmatrix} 150 & 0 \\ 0 & 1 \end{pmatrix}. \tag{20}$$

The total number T of target-tracking steps is the same for all the simulations and fixed at $T = 50$ and the radar position will be always at $s = [0, 0]$, for the sake of simplicity and indeed w.l.o.g. in the application of the filters. The time step and the glint noise occurrence probability will be chosen accordingly to the specific scenarios, allowing to perform the process of validation of the results with different boundary conditions. Regarding the Particle Filters (PFs), the number of particles is chosen as $N_s = 500$ for all the simulations, in order to keep a suitable and comparable computation time, which is found to be the main drawback in the application of such methodologies. The PF algorithm is implemented making use of the sequential importance sampling procedure, whilst an output injection gain matrix L of the FQF is such that $A - LC$ has eigenvalues $\{0.4730, 0.4620, 0.4510, -0.4400, 0.4500, 0.4000\}$ (see [13] for details). The numerical results will be compared according to the standard relative position errors (RPEs). It is defined for a noise realization i at time k as:

$$RPE_i(k) = 100 \cdot \sqrt{\frac{\hat{e}_1^{(i)}(k)^2 + \hat{e}_4^{(i)}(k)^2}{x_1^2(k) + x_4^2(k)}} \tag{21}$$

where $\hat{e}_j^{(i)}(k) = x_j(k) - \hat{x}_j^{(i)}(k),\ j = 1, 4$ with $\hat{x}_1^{(i)}(k)$ and $\hat{x}_4^{(i)}(k)$ being respectively the estimated position on the $x-axis$ and on the $y-axis$ at time k. Also, computational time is shown. It is finally necessary to point out that all the results will consist of a mean of 50 Monte Carlo runs.

The first scenario will consist in testing the reaction of each filter to different choices of the time step τ, in particular three scenarios for each filter will be built for a total of twelve scenarios. It is naturally expected that the performance will decrease proportionally to the increasing of the time step, so that this scenarios are drawn in order to underline the robustness of the methods to more and more challenging situations dictated by different radar settings. For these first scenarios, the glint noise probability is always chosen as $\varepsilon = 5\%$. The results show the superiority of the FQF with virtual measurements with respect to the other filters under all the three conditions. It is worth noticing how the Markov Chain Monte Carlo (MCMC) improves the reliability of the PF, yet indeed it depends on the application whether the performance may be considered enough or not to justify the increase in complexity. It is finally evident how the Interacting Multiple Model (IMM) filter has the important downside of decreasing its performance at higher values of the time step τ, which indeed holds true also for the FQF implementation, yet for the PF methods the decrease in performance is almost negligible, showing the interest on applying likelihood-based methods.

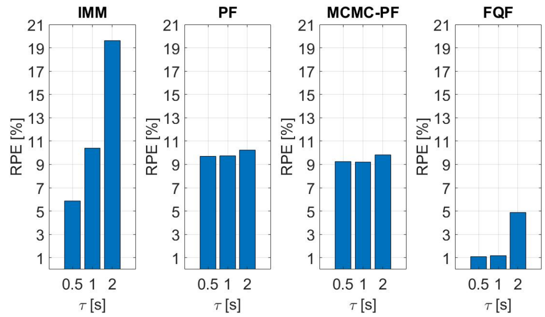

Fig. 2. RPE values for each filter varying time step τ, 2D case.

The second scenario has been developed to draw conclusions which have as a main aim to check the robustness of the methods with respect to wrong assumptions over the glint noise parameters. In particular, in this section it will be checked the reaction of the filters under different values of the glint noise probability ε. Thus, the simulations are carried fixing the time step at $\tau = 1$s and for three values of the glint noise probability. The results show also that, even if there is a clear variation on the error of the other filters, the solutions are still indeed acceptable and, most importantly, the errors of all the filters keep staying under the values returned by the IMM filter. Finally, as the first scenario, also in this case the Quadratic Filter is shown to be dominant.

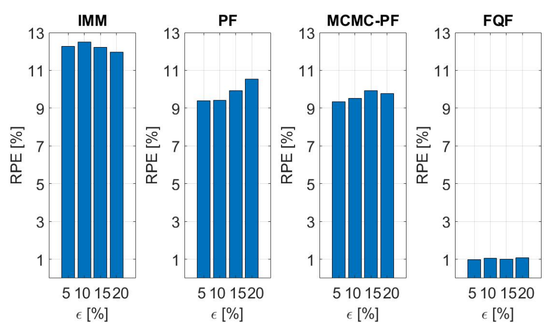

Fig. 3. RPE values for each filter varying glint noise probability ε.

As a last glimpse to the filters' behaviours in the two-dimensional space, the computational times are compared. A renowned feature of the IMM methodology is its computational speed, so that it is expected to behave well in this scenario. Vice versa, the computational complexity in the evaluation of the evolution of the particles and the re-sampling step are a severe computational burden in the evaluation of a solution for the PF methodologies.
The results shown in the table show that the evaluation time for the FQF is a good trade-off among the IMM and the PF methods.

IMM	PF	MCMC-PF	FQF
0.006966s	0.032208s	0.070264s	0.008574s

TABLE I
COMPUTATIONAL TIMES TABLE [SECONDS].

B. Numerical simulations: 3D target tracking

Here the matrix L is chosen in each simulation such that the eigenvalues are moved to $\rho(A) = \{0.4730, 0.4620, 0.4510, 0.4400, 0.4555, 0.4420, 0.4660, 0.4566, 0.4860\}$, whereas the IMM, the PF and the MCMC-PF are developed under the same design choices of the previous chapter concerning the problem in two dimensions. The initial state is now set to be defined as:

$$x_0 = \left[1000, -5, 0, -1000, 5, 0, 2000, -5, 0\right]^\top . \tag{22}$$

The glint noise covariance matrices are now specified adding the value of the variance on the bearing angle noise, which is considered to be equal to the one acting on the polar angle. In particular, the covariance matrix for the background Gaussian measurement noise and the glint-noise matrix covariance are

$$\Sigma_g = \begin{pmatrix} 5 & 0 & 0 \\ 0 & 0.1 & 0 \\ 0 & 0 & 0.1 \end{pmatrix} \quad \Sigma_l = \begin{pmatrix} 150 & 0 & 0 \\ 0 & 1 & 0 \\ 0 & 0 & 1 \end{pmatrix}. \tag{23}$$

Again, total simulation steps and radar position are set respectively to $T = 50$ and $s = [0\text{m}, 0\text{m}]$.
The RPE is now defined as:

$$RPE_i(k) = 100 \cdot \sqrt{\frac{\hat{e}_1^{(i)}(k)^2 + \hat{e}_4^{(i)}(k)^2 + \hat{e}_7^{(i)}(k)^2}{x_1^2(k) + x_4^2(k) + x_7^2(k)}} \tag{24}$$

where $\hat{e}_j^{(i)}(k) = x_j(k) - \hat{x}_j^{(i)}(k),\ j = 1, 4, 7$ with $\hat{x}_1^{(i)}(k)$, $\hat{x}_4^{(i)}(k)$ and $\hat{x}_7^{(i)}(k)$ being respectively the estimated position on the $x - axis$, on the $y - axis$ and on the $z - axis$ at time k.
The first scenarios which will be investigated will deal with the comparison of the results of the four filters made on a basis of different choices of the time steps, which will follow the same design choices of the first scenarios of the previous section. The results still follow the conclusions drawn in the previous section, proving a superiority of target tracking developing the Feedback Quadratic Filter methodology. Differently from the bi-dimensional case, a few non-convergent runs (*i.e.* $RPE(k) > 30\%$) occurred, especially for the application of the Feedback Quadratic Filter for $\tau = 2$s, which counts a total of 10 non-convergent Monte Carlo runs. The reason may be found in the fundamental principle of the FQF algorithm which is the challenging application to systems which are not internally stable. In other applications the number of non-convergent runs does not count a total of more than 3 non-convergent runs.

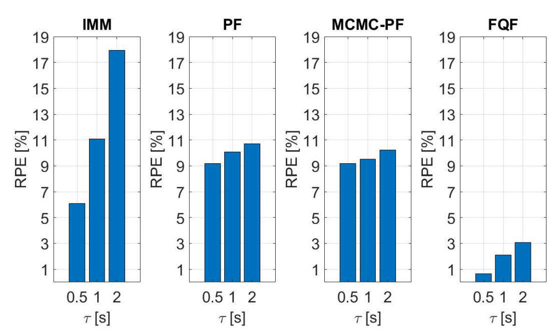

Fig. 4. RPE values for each filter varying time step τ, 3D case.

A second scenario is developed to show the robustness to higher values of the glint noise covariance matrix, which is indeed the case for closer to-be-tracked objects. The time step is now fixed at $\tau = 0.5$s, for which the MCMC-PF and the PF filters were showing the most similar behaviour, and the glint noise occurrence probability is fixed at $\varepsilon = 5\%$ for all the simulations. The new glint noise covariance matrix Σ_l^{new} is now defined as $\Sigma_l^{new} = 2 \cdot \Sigma_l$.

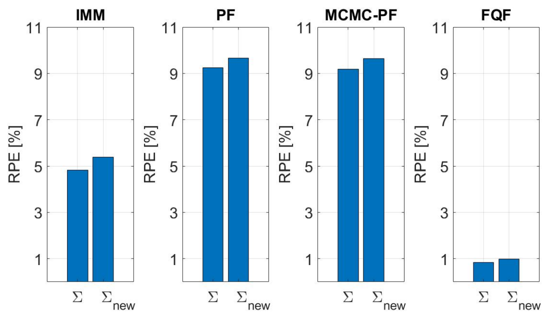

Fig. 5. RPE values for each filter varying measurement glint noise covariance.

Finally, it is shown again the computational time of each filter for a random step in $\{1, T\}$ of the algorithm and a random Monte Carlo run in the following table:

IMM	PF	MCMC-PF	FQF
0.013534s	0.123702s	0.165724s	0.050230s

TABLE II
COMPUTATIONAL TIMES TABLE, 3D CASE [SECONDS].

V. CONCLUSIONS

A solution to the problem of the 2D and 3D target tracking in the presence of heavy tailed noise (and in particular in the case of the glint noise) is given in this paper. Several combinations of the problem parameters were interchanged, in order to stress the filters under different conditions. Numerical simulations and comparisons with standard methods in a case of study validate the proposed approach. Further extensions can include the study of other and complex target dynamics, multi-agents case in a cooperative/distributed filtering framework ([22], [23]), packet dropping scenarios ([24], [25]), learning-based approaches ([26], [27]), delayed measurements ([28], [29]), analysis in Hamiltonian framework ([30]). Another pioneering development could be the extension of the presented technique to infinite-dimensional systems ([31]).

REFERENCES

[1] G. M. Siouris, Missile guidance and control systems, Springer Science & Business Media, 2004.
[2] C. Masreliez, Approximate non-Gaussian filtering with linear state and observation relations, IEEE Transactions on Automatic Control 20 (1) (1975) 107–110.
[3] C. Masreliez, Ph.d dissertation: Robust recursive estimation and filtering, University of Washington, Seattle (1972).
[4] G. A. Hewer, R. D. Martin, J. Zeh, Robust preprocessing for Kalman filtering of glint noise, IEEE Transactions on Aerospace and Electronic Systems AES-23 (1) (1987) 120–128.
[5] I. Bilik, J. Tabrikian, Maneuvering target tracking in the presence of glint using the nonlinear Gaussian mixture kalman filter, IEEE Transactions on Aerospace and Electronic Systems 46 (1) (2010) 246–262.
[6] I. Bilik, J. Tabrikian, Target tracking in glint noise environment using nonlinear non-gaussian kalman filter, in: 2006 IEEE Conference on Radar, IEEE, 2006, pp. 6–pp.
[7] J. Zhang, H. Ji, Q. Xue, A new approach based on particle filter for target tracking with glint noise, in: 2009 IEEE International Conference on Systems, Man and Cybernetics, IEEE, 2009, pp. 4791–4795.
[8] H. Hongtao, J. Zhongliang, L. Anping, T. Hongwei, Target tracking in glint noise using a MCMC particle filter, Journal of Systems Engineering and Electronics 16 (2) (2005) 305–309.
[9] H. Du, W. Wang, L. Bai, Observation noise modeling based particle filter: an efficient algorithm for target tracking in glint noise environment, Neurocomputing 158 (2015) 155–166.
[10] J. Kim, M. Tandale, P. K. Menon, E. Ohlmeyer, Particle filter for ballistic target tracking with glint noise, Journal of guidance, control, and dynamics 33 (6) (2010) 1918–1921.
[11] H.-W. Li, J. Wang, Particle filter for manoeuvring target tracking via passive radar measurements with glint noise, IET Radar, Sonar & Navigation 6 (3) (2012) 180–189.
[12] W.-R. Wu, Maximum likelihood identification of glint noise, IEEE transactions on aerospace and electronic systems 32 (1) (1996) 41–51.
[13] S. Battilotti, F. Cacace, M. d'Angelo, A. Germani, The polynomial approach to the LQ non-Gaussian regulator problem through output injection, IEEE Transactions on Automatic Control 64 (2) (2018) 538–552.
[14] F. Cacace, F. Conte, M. d'Angelo, A. Germani, Feedback polynomial filtering and control of non-Gaussian linear time-varying systems, Systems & Control Letters 123 (2019) 108–115.
[15] F. Cacace, F. Conte, M. d'Angelo, A. Germani, Filtering of systems with nonlinear measurements with an application to target tracking, International Journal of Robust and Nonlinear Control 29 (14) (2019) 4956–4970.
[16] M. I. Skolnik, Radar handbook, McGraw-Hill Education, 2008.
[17] M. I. Skolnik, et al., Introduction to radar systems, Vol. 3, McGraw-hill New York, 1962.
[18] D. M. Patterson, R. A. Ashley, Glint tracking errors in radar, in: A Nonlinear Time Series Workshop, Springer, 2000, pp. 121–136.
[19] T. L. Song, D. G. Lee, Effective filtering of target glint, IEEE Transactions on Aerospace and Electronic Systems 36 (1) (2000) 234–240.
[20] B. D. O. Anderson, J. B. Moore, Optimal filtering, Courier Corporation, 2012.
[21] X. R. Li, V. P. Jilkov, Survey of maneuvering target tracking: Iii. measurement models, in: Signal and Data Processing of Small Targets 2001, Vol. 4473, International Society for Optics and Photonics, 2001, pp. 423–446.
[22] S. Battilotti, F. Cacace, M. d'Angelo, A. Germani, Cooperative filtering with absolute and relative measurements, in: 2018 IEEE Conference on Decision and Control (CDC), IEEE, 2018, pp. 7182–7187.
[23] S. Battilotti, F. Cacace, M. d'Angelo, A stability with optimality analysis of consensus-based distributed filters for discrete-time linear systems, Automatica 129 (2021) 109589.
[24] S. Battilotti, F. Cacace, M. d'Angelo, A. Germani, B. Sinopoli, LQ non-Gaussian regulator with Markovian control, IEEE Control Systems Letters 3 (3) (2019) 679–684.
[25] S. Battilotti, F. Cacace, M. d'Angelo, A. Germani, B. Sinopoli, Kalman-like filtering with intermittent observations and non-Gaussian noise, IFAC-PapersOnLine 52 (20) (2019) 61–66.
[26] S. Xu, Y. Ou, X. Wu, Learning-based adaptive estimation for aoa target tracking with non-gaussian white noise, in: 2019 IEEE International Conference on Robotics and Biomimetics (ROBIO), IEEE, 2019, pp. 2233–2238.
[27] V. De Iuliis, G. D. Di Girolamo, F. Smarra, A. D'Innocenzo, A comparison of classical identification and learning-based techniques for cyber-physical systems, in: 2021 29th Mediterranean Conference on Control and Automation (MED), IEEE, 2021, pp. 179–185.
[28] V. De Iuliis, A. Germani, C. Manes, Identification of forward and feedback transfer functions in closed-loop systems with feedback delay, IFAC-PapersOnLine 50 (1) (2017) 12847–12852.
[29] S. Battilotti, M. d'Angelo, Stochastic output delay identification of discrete-time Gaussian systems, Automatica 109 (2019) 108499.
[30] A. Moreschini, M. Mattioni, S. Monaco, D. Normand-Cyrot, Stabilization of discrete port-hamiltonian dynamics via interconnection and damping assignment, IEEE Control Systems Letters 5 (1) (2020) 103–108.
[31] F. Cacace, M. d'Angelo, V. De Iuliis, A. Germani, Filtering discrete-time systems with multiplicative noise in L_2 spaces with applications, IEEE Control Systems Letters (2021).